CHARACTERISTICS OF PEMFC OPERATION IN AMBIENT AND LOW PRESSURE ENVIRONMENT CONSIDERING THE FUEL CELL HUMIDIFICATION

C. Werner [a], F. Gores [a], L. Busemeyer [a], J. Kallo [b], S. Heitmann [c], M. Griebenow [c]

[a] German Aerospace Center, Institute of Engineering Thermodynamics, Hein-Saß-Weg 38, 21129 Hamburg
[b] German Aerospace Center, Institute of Engineering Thermodynamics, Pfaffenwaldring 38-40, 70569 Stuttgart
[c] University of Hamburg, Lothar Collatz Center for Computing in Science, Bundesstraße 55, 20146 Hamburg

SUMMARY

This paper summarizes experimental results of an air fed polymer electrolyte membrane fuel cell system HyPM XR 12 (Hydrogenics Corp.) considering fuel cell temperature, stoichiometry and load requirement variations at ambient and low pressure operation. The experimental work realized at a low pressure test facility designed and assembled by the German Aerospace Center, Institute of Engineering Thermodynamics is based on an experimental design.
The experimental results confirm reduced fields of fuel cell operation as well as a decreased gross stack performance and efficiency at low operating pressures (950 mbar ≥ p ≥ 600 mbar) for defined fuel cell temperature, stoichiometry and load requirement. In addition, indexes of the operating parameters are introduced characterizing the fuel cell operation with regard to the gross stack performance and efficiency at ambient and low pressure level. The discussion of the results considers analyses of fuel cell humidification.

KEYWORDS

1. INTRODUCTION

Air fed fuel cells meet variable environmental pressure levels from 700 to 1000 mbar[1)] in regular aircraft operation. The variation of the system pressure results in changes of current-voltage-characteristic (cp. Figure 1) and fuel cell performance, consequently. The expected change of the current-voltage-characteristic is due to the oxygen partial pressure variation at varying total pressure on the one hand. The oxygen partial pressure affects the fuel cell voltage according to the Nernst equation and is conditionally adjustable, inter alia by the cathode stoichiometric ratio.

On the other hand, the current-voltage-characteristic is influenced by the water-holding capacity depending on the total pressure of air within the cathode. The resulting humidity inside the fuel cell defines the membrane resistance and ohmic loss accordingly. The cell humidity is adjustable by setting temperature and/or cathode stoichiometric ratio [22-23].

These correlations and further effects of total operating pressure variation in polymer electrolyte membrane fuel cells (PEMFC) on performance, educt demand and distribution, water generation as well as auxiliary energy demand are described by [1-8]. According to [6] a decrease of the system pressure from p_{amb} to $p <$ p_{amb} (AC requirements) results in decreased system efficiency. The relevance of the parameter combination fuel cell temperature/load requirement or stoichiometry/load requirement on performance in non-super-charged and supercharged PEMFC is discussed in [5, 11-18] in addition.

[1)] Reference: Cruise (700 mbar) and ground operation (1000 mbar). Pressure in emergency operation down to 200 mbar (cp. cabin decompression) [9].
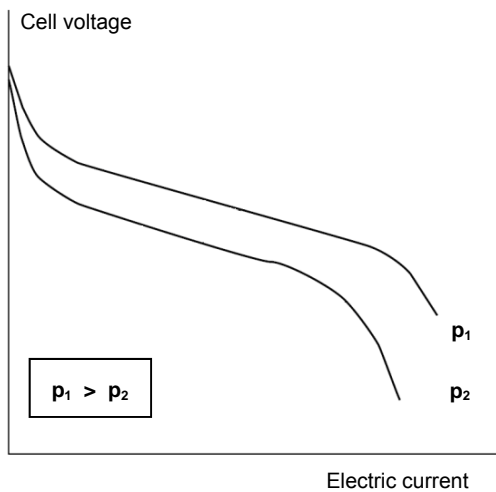
Fig. 1 Current-voltage-characteristic of a fuel cell depending on system pressure [8]

This paper aims at the performance and efficiency of a PEMFC system described qualitatively and quantitatively by means of experimental data. The focus is on fuel cell system operation at $p < p_{amb}$ (AC requirements) and approved reproducible parameter combinations. The operating pressure, fuel cell temperature, stoichiometry and load requirement of an air fed PEMFC system HyPM XR 12 are varied systematically during experimentation on the basis of an experimental design to determine the approvable parameter combinations (operating fields) and to define the operating fields of the PEMFC system. Moreover, fuel cell temperature, stoichiometry and load requirement are characterized concerning their impact on the cell humidification and consequently on the performance and efficiency at ambient pressure operation $p = p_{amb}$ and low pressure operation $p < p_{amb}$ of the PEMFC system.

2. EXPERIMENTS ON PEMFC OPERATION

The PEMFC operation at $p \leq p_{amb}$ was investigated detailed at the German Aerospace Center, Institute of Engineering Thermodynamics. The low pressure test facility developed for PEMFC systems as well as the experimental procedure will be described within the following subsections.

2.1. Description of the low pressure test facility for PEMFC systems

The low pressure test facility for PEMFC systems was designed and assembled by the German Aerospace Center, Institute of Engineering Thermodynamics. Due to its modular construction it is a flexible and extensible facility to characterize the operation of PEMFC and subcomponents, e.g. condensers, dryers or power electronics. The general specification is given in Table 1.

Tab. 1 General specification of the low pressure test facility for PEMFC systems

mass flow (cathode)	≤ 2500 slpm
mass flow (anode purge)	≤ 25 slpm
operating pressure	p_{amb} -200 mbar
cooling capacity	30 kW
electric capacity	25 kW
operating temperatures	10-70 °C

The principle process diagram of the low pressure test facility is shown in Figure 2. The vacuum pumps installed at the system output generate the low pressure level inside the fuel cell system by suction operation

at $p = p_{amb}$, as well as $p < p_{amb}$. Except from the operating pressure, the parameters fuel cell temperature, stoichiometry and load requirement can be adjusted continuously at the test facility.
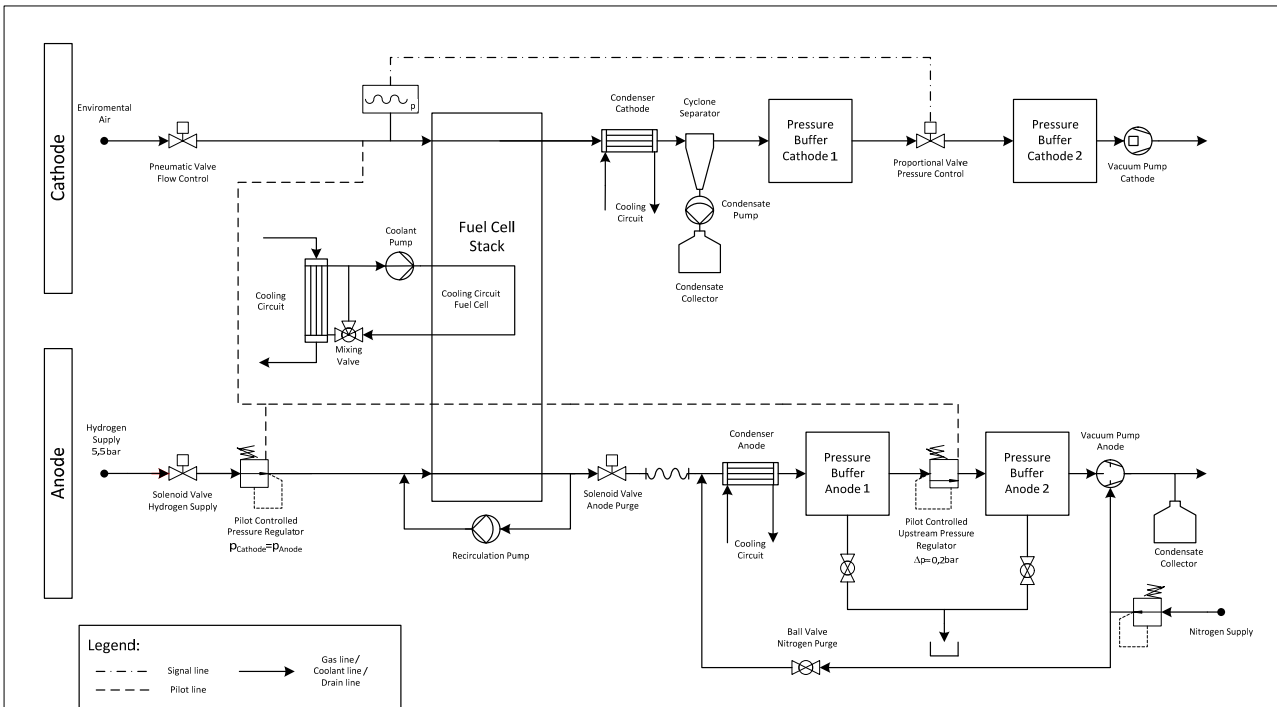

Fig. 2 Principle process scheme of the low pressure test facility for PEMFC designed and assembled by the German Aerospace Center, Institute of Engineering Thermodynamics

PEMFC system: A fuel cell module manufactured by Hydrogenics Corp. (Type: HyPM XR12) is used for the low pressure experiments. The module contains the fuel cell stack as well as auxiliary units including electronic control system, solenoid valves, coolant pump, recirculation pump and pressure regulator. The general specification of the stack is summarized in Table 2.

Tab. 2 General specification of the fuel cell stack

rated power	12 kW
number of cells	60
active (total-)surface per cell	496 cm²
maximal current (output)	350 A
voltage (output)	30-60 V
flow field	multi-meander
membrane	Nafion®
catalyst load	0.3 mg Pt/cm²

Cathode: The air mass flow (ambient air) for fuel cell operation is provided by a pneumatic control valve at system input. The water generated inside the fuel cell is collected by a condenser (plate heat exchanger) and a cyclone separator located at the stack outlet. A pump is applied to drain the cyclone separator. The pressure signal at stack input is used as reference value for pressure control and adjusts the proportional valve at system output. The low pressure level inside the test facility is realized by a vacuum pump (claw compressor with a high volume rate).

Anode: The hydrogen pressure at stack input is regulated with reference to the pressure at cathode inlet.

This is realized by a mechanical pressure regulator. The pressure dome of this pressure regulator refers to the cathode room via pilot line. A solenoid valve is installed at stack output to purge the dead end system with internal hydrogen re-circulation in periodic load dependent intervals. The low pressure generator of the anode is located downstream the fuel cell module. In low pressure operation, the output pressure downstream the purge valve is set about 200 mbar below the stack pressure by a mechanical upstream pressure regulator, which is pilot-controlled by the cathode pressure as well. A liquid-cooled condenser unit protects the subsequent sensors and the vacuum compressor from high moisture loads. A vacuum pump (oil-sealed rotary-vane pump) supplying the unregulated vacuum is installed after the upstream pressure regulator and the pressure puffer.

Gas supply: Separated low pressure generators were developed at cathode and anode string to guarantee a safe and flexible operation. The gas flows are strictly divided. A mechanically communicating vacuum control between anode and cathode ensures a permanently minor pressure difference between the membranes.

Cooling system: The stack cooling is connected with the central cooling supply of the fuel cell laboratory via plate heat exchangers. The temperature control is realized by a mixing valve in the primary cooling circuit. A separated reciprocator chiller supplies the condensers of the cathode and anode string to meet the low temperature level required.

Electronic load: The electric power supplied by the fuel cell system is controlled by the electric load. The electric load can be separated from the system via high current contactors to ensure a quick shutdown in case of system failures.

Sensors: The low pressure test facility includes 80 sensors to register the input- and output variables of the tested fuel cell system (pressure, temperature, concentration, humidity, mass flow, current, voltage) and the environmental conditions (pressure, temperature, oxygen concentration and relative humidity) during the experiments.
Mass flow, temperature, pressure, relative humidity and oxygen concentration are recorded inside the cathode string before stack and after condensation. In addition, temperature and pressure are determined between stack and condensation. Furthermore, the exhaust air of the cathode is analyzed in terms of hydrogen. The hydrogen mass flow is analyzed inside the anode string. Therefore, hydrogen concentration and relative humidity are ascertained. Pressure sensors and an overpressure switch are applied at anode stack input and inside the low pressure generating unit after the purge valve as well as in the vacuum part. The input and output temperatures as well as the coolant mass flow are recorded to prove cooling and condensation.

Control and data collection: The analogue signals of the sensors are transferred via A/D converter onto a CAN-Bus system and a data logger. The recorded and scaled data are transferred via Ethernet to a PC. A Matlab/Simulink model [22] developed is used to control the system. An industrial PC is applied for the implementation of the system control. The operating interface created in Simulink is located on a separate PC to control and to present all relevant operating parameters of the fuel cell, the peripheral components and the low pressure generators in online-graphs.

2.2. Test procedure

The operating parameter variations of the PEMFC are realized within defined intervals for the experimental research (Table 3). These intervals result from the specifications of the fuel cell system investigated and the operation requirements in aviation.

Tab. 3 Description of the parameters examined

Parameter	Parameter values
operating pressure p (stack input)	600 mbar; 700 mbar; 800 mbar; 900mbar; 950 mbar
cooling temperature t (stack output)	45 °C; 50 °C; 55 °C; 60 °C; 65 °C
stoichiometry λ (cathode)	1.7; 1.9; 2.1; 2.3; 2.5
load requirement I (electrical current)	50 A; 150 A; 250 A; 300 A; 350 A

The measurements aim at determining the connection between the four input variables (operating parameters), viz. operating pressure p, cooling temperature t, stoichiometry λ, load requirement I and the dependent variables, viz. gross stack performance $P_{Stack,Gross}$ and efficiency η_u. In order to consider the complete measurement phase space of operating parameters with the step size from Table 3, $5^4 = 625$ separate measurements are required. This number is not feasible. Reduced measurement effort may be realized by using experimental design [19].
This statistical method allows deriving the optimal points in the measurements phase space for a prescribed number of measurements. It determines the dependent variables as simple functions of the input variables, namely as polynomials. The coefficients of the polynomials are purely data-driven, i.e. they are estimated by linear regression on the experimental results. The points in measurements phase space are called ‚D-optimal‘ if the determinant of the corresponding information matrix is maximized. Here, the information matrix J depends on the points in measurements phase space. In order to introduce the information matrix, the general regression problem is to be considered

(1) $\min \| y\text{-}Mx \|_2 \qquad$ with $x \in R^m$

$M \in R^{m,n}$ is the design matrix, x the vector of coefficients, n the number of coefficients, $y \in R^m$ the target variable, m the number of experiments and $\|.\|_2$ the Euclidian norm. The solution of this problem is given by

(2) $x = \left(M^{'} \cdot M \right)^{-1} \cdot M^{'} \cdot y$

The corresponding information matrix is given by

(3) $J = M^{'} * M.$

Increasing the determinant of J results in a more precise estimation of the parameters x [19]. The operating points of the PEMFC to be tested are calculated by the Matlab [20] algorithm ’candexch‘ creating a D-optimal experimental design. From a mathematical point of view, the regression model is an estimation of the Taylor polynomial of degree four around the normalized ‚0-point‘ where p = 775 mbar; t = 55 °C; λ = 2.1; I = 132 A. Some of the higher-order interaction terms have been dropped (Appendix, Table 11).The statistical model thus serves (i) as an a priori guiding to allow a reduced number of experiments and (ii) as a compact tool to represent the experimental findings a posteriori while accounting for measurement uncertainty.
The prescribed number of measurements in the test plan is initially chosen as 150, being only about ¼ of the required 5^4=625 measurements. 133 test points are supposed to determine the model coefficients while further 17 test points are selected to validate the test results a posteriori. Within the 133 test points the ‚0-point‘ is considered three times to record drift behavior during experimentation.
However, in the course of experiments it turns out that steady operation at the low pressure fuel cell test facility cannot be realized in some a priori chosen test points (Appendix, Table 11). The algorithm is applied repeatedly to calculate a new test plan incorporating already realized points within a smaller set of admissible test points. Some more test points are added manually in order to cover the interesting region of low pressure conditions. Thus, the final number of test points amounts to 169.
Figure 3 shows the distribution of test points of the D-optimal algorithm using the example of λ = 2.1 and t = 45 °C. Figure 3 includes nine test points to be measured once and three test points to be measured twice. Those points to be measured twice are called ‚Double test‘ points. The experimental design algorithm considers them as statistically especially relevant.
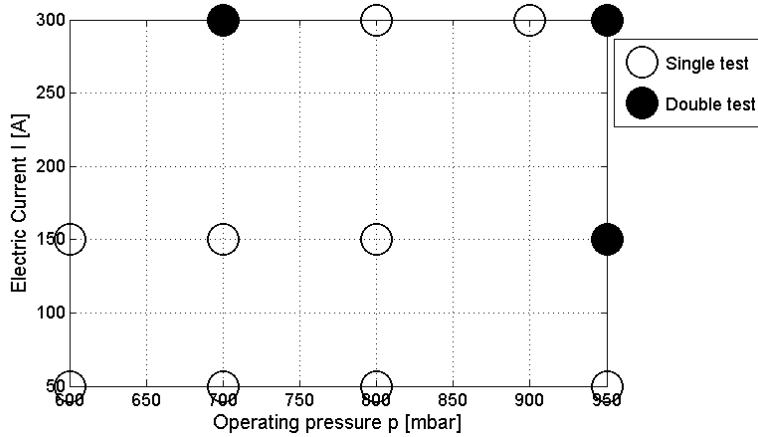
Fig. 3 Detail of the experimental design for PEMFC experimentation, (reference: λ = 2.1; t = 45 °C)

3. RESULTS

Global measures, such as the coefficient of determination and the standard deviation indicate a sufficient approximation of the measured variables. This holds for the dependent variable $P_{Stack,Gross}$ where the coefficient of determination R^2 = 0.9953 and the standard deviation σ = 273.2 W and the dependent variable η_u where the coefficient of determination R^2 = 0.9585 and the standard deviation σ = 0.0167. Hence, the relative mean error amounts to about 3 % in both variables. However, the complete regression model generates non monotonous graphs. One example is the gross stack performance which is expected to increase monotonically as a function of the operating pressure. Non-monotone behavior is physically implausible and may be considered a numerical artifact attributable to high-order polynomial regression. Figure 8 (a) displays an example where the unexpected decrease of performance with increasing pressure is already present in the experimental data. The non-monotone behavior of the regression model is therefore at least partially induced by (some of) the measurements. Consequently, significant deviations between the regression curves and the measured data are ascertainable in some regions of the parameter space. For this reason, the complete regression model is replaced by a local quadratic model in the following analysis. 'Local quadratic' means that a quadratic model is used in any partial experimental region (plane), i.e. two operating parameters are fixed and two operating parameters are variable in any partial experimental plane. All measuring points located in the particular planes (cp. Figure 8, 9 and 10) are used to determine the coefficients of the local quadratic model. For this reason, statements about the connections between operating variables and the dependent variable can be concluded inside the particular planes only (defined by the references stated below the figures).

The following statements, based on the mathematical model for evaluation of experiments, concern the operating field and the effects of the input variables (operating parameters) on the dependent output variables of the fuel cell system HyPM XR 12. The regression curves, shown in Figure 6-7, are computed from all measuring points located in the depicted measuring area. Therefore, there is only one regression function per figure. The model was specified to enable valid statements in strongly restricted operating fields (cp. Figure 8, t = 65 °C). The reference point in Table 4 is defined as an example of use to illustrate the results for the (admissible) low pressure operation.

Tab. 4 Definition of the reference point

operating pressure (stack input) p	700 mbar / 950 mbar
cooling temperature (stack output) t	45 °C
stoichiometry (cathode side) λ	2.1
load requirement (electric current) I	300 A

6

3.1. Operating fields of PEMFC systems

Admissible and non-admissible operating areas were identified for 600 mbar ≤ p ≤ 950 mbar depending on cooling temperature at stack output, stoichiometry and load requirement (Figure 4 a-c). The operating field (admissible operating area) narrows at decreasing operating pressures for the reference defined. Combinations of low operating pressures and high cooling temperatures at stack output or high cathode stoichiometric ratios or high load requirements are excluded from the fuel cell operation for constraints given in Figure 4 a-c, since the operating parameter combinations mentioned affect the resulting cell voltage and result in a non-steady fuel cell operation at the low pressure test facility. It has to be noted, that the admissible operating area may also be partially limited by the test facility. For instance, the resulting high volume flows exceed the capacity of the vacuum compressor in operating areas characterized by low absolute pressures and high mass flows (resulting from high loads and stoichiometric ratios) due to the decreased density of the process gas. The total number of steady operating points amounts to 363 of 625 measuring points originally (cp. full factorial experimental design).
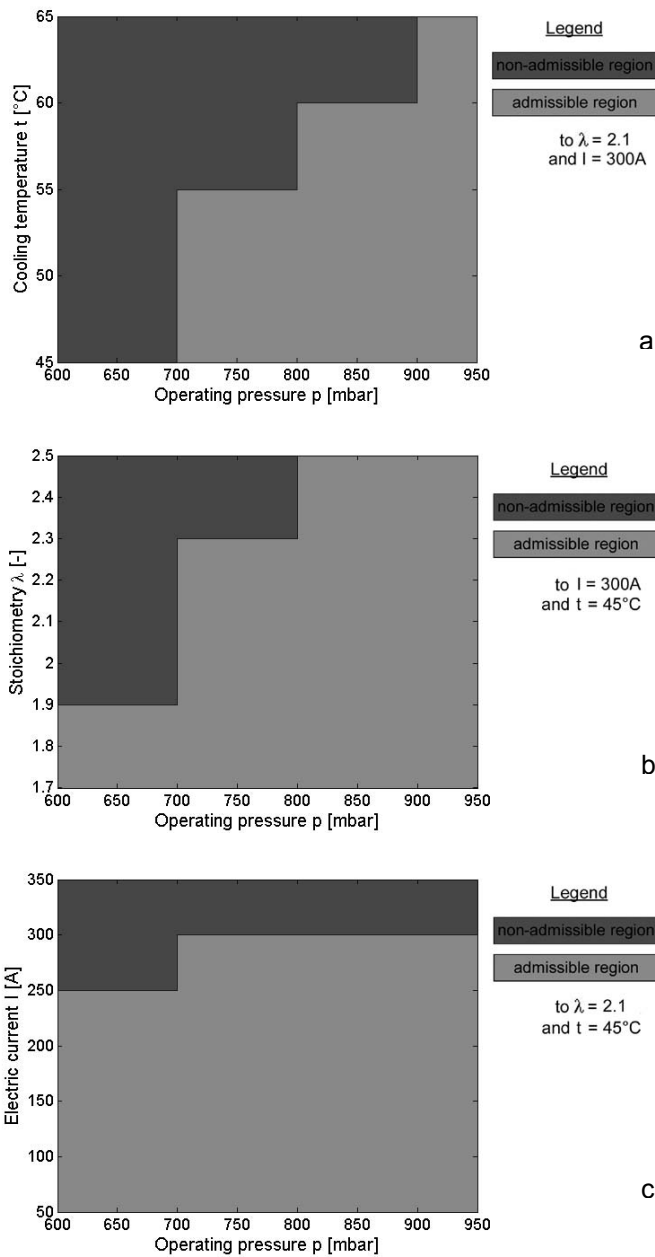

Fig. 4 PEMFC operating fields depending on the operating pressure (a-c)

3.2. Characteristics of PEMFC operation

In this subsection, the gross stack performance and efficiency (average cell efficiency) is used to evaluate the fuel cell system operation at ambient and low pressure level. The analysis considers the humidification of the fuel cells. Therefore the dew point temperature depending on the cathode stoichiometric ratio and the operating pressure is introduced.

The electrical gross stack performance $P_{Stack,Gross}$ is calculated on the basis of the current provided by the stack feeding the public grid I_{Net}, the current provided by the stack supplying the auxiliary components I_{BOP} (BOP: balance of plants, e.g. cooling pump, recirculation pump, control electronics, solenoid valves) and the total voltage of the fuel cell stack U_{Stack}:

(4) $P_{Stack,Gross} = (I_{Net} + I_{BOP}) \cdot U_{Stack}$

The measured average cell voltage U(I), the existing number of cells n and the reversible cell voltage U_0 are considered to calculate the average cell efficiency according to [10].

(5) $\eta_U = \dfrac{U(I)}{n \cdot U_0}$

The reversible cell voltage U_0 results from the variation of the Gibbs free enthalpy ΔG^0 or the variation of the enthalpy of formation ΔH^0 and the product of temperature and variation of the reaction entropy ΔS^0 as well as the number of electrons z in the redox reaction and the Faraday constant F (cp. equation 6).

(6) $U_0 = -\dfrac{\left(\Delta G^0\right)}{zF} = -\dfrac{\left(\Delta H^0 - T\Delta S^0\right)}{zF}$

The parameters mentioned are affected significantly by several operating parameters, such as oxygen partial pressure and fuel cell humidification discussed below. The optimum of the relative humidity rH is achieved at rH ≈ 100% at the outlet of the cathode [8], meaning that the temperature at the outlet of the cathode is close to the dew point temperature. The correlation between cathode stoichiometric ratio, operating pressure and dew point temperature is described by [8, 22].

(7) $p_W = \dfrac{(0.420 + \psi \cdot \lambda) p_{out}}{(1+\psi) \cdot \lambda + 0.210}$ with $\psi = \dfrac{p_{W,in}}{p_{in} - p_{W,in}}$

The vapor pressure of water p_w at cathode outlet considers the cathode stoichiometric ratio λ, the total pressure at fuel cell inlet p_{in} as well as the vapor pressure of water at fuel cell inlet and the total pressure at fuel cell outlet p_{out} [8]. Equation 8 describes the dew point temperature at cathode outlet based on water vapor pressure according to [22].

(8) $t_{dew} = -2.581E^{-18} \cdot (p_W)^4 + 6.4056E^{-13} \cdot (p_W)^3 - 5.8916E^{-8} \cdot (p_W)^2 + 2.8427E^{-3} \cdot (p_W) + 2.2455E^{+1}$

The relative humidity rH at cathode outlet is described by the vapor pressure of water p_w (cp. equation 7) and the saturation pressure p_{sat} at corresponding temperature tabulated in [24].

(9) $rH = \dfrac{p_W}{p_{sat}}$

Figure 5 is based on equation 7 and 8. It illustrates the dew point temperatures depending on cathode stoichiometric ratios in ambient pressure operation (950 mbar) and low pressure operation (700 mbar). The following constraints are assumed for calculation:

- the inlet air is controlled in terms of temperature (t = 20 °C) and relative humidity (rH = 60 %)
- the pressure of the inlet air is set to 700 mbar or 950 mbar, respectively
- pressure drop between cathode inlet and outlet is neglected
- the net drag in consequence of the water transport from cathode to anode is neglected.
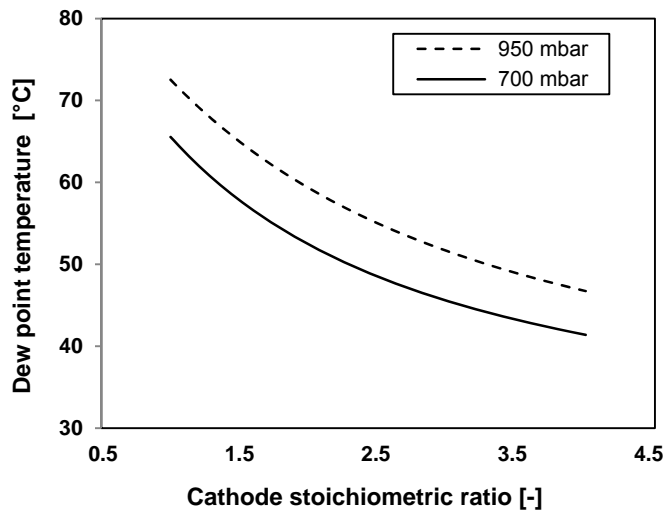 All the water remains at cathode side until leaving the fuel cell stack along with the exhaust gas.

Fig. 5 Dew point temperature depending on cathode stoichiometric ratio and operating pressure referred to [8, 22]

Figure 5 proves a decrease of dew point temperature at decreasing operating pressure. Consequently, the lower the operating pressure the dryer the air at a defined temperature. Furthermore, an increase of the cathode stoichiometric ratio at a certain operating pressure results in a decrease of the dew point temperature and a dehumidification of air inside the fuel cell stack at a defined temperature (Figure 5).
Accordingly, decreased operating pressure demands decreased stack temperature (cp. cooling temperature in Table 3) to achieve the same membrane humidity inside the fuel cell stack. Furthermore, an increased cathode stoichiometric ratio at a defined operating pressure requires decreased stack temperature as well to realize the same membrane humidity inside the fuel cell stack.

Figure 6 illustrates the experimental data of the gross stack performance and the efficiency as well as corresponding regression functions with respect to the defined parameters from section 3. The correlation of the gross stack performance or the efficiency and operating pressure of the fuel cell system is presented. The decrease of the gross stack performance and the efficiency is attributable to the decreasing oxygen partial pressure. The fuel cell humidification affecting the membrane resistance is given in any case (Table 5) [2]. A cell flooding at operating pressures p_cathode_out (measured) ≥ 680 mbar is ascertained yet according to Table 5, even though a steady fuel cell operation (below the dew point temperature) is realized. The present example proves a decrease of gross stack performance and efficiency of 5.3 %, when reducing the operating pressure from p = 950 mbar to p = 700 mbar. The standard deviation is 113.7 W (gross stack performance) and 0.006 (efficiency) within the operating pressure area discussed (700 - 950 mbar).

---

[2] The evaluation of the fuel cell humidification for the measuring points in Table 5-8 is based on the relative humidity rH calculated for the PEMFC parameters examined. The classification "dry" (rH < 90 %), "adequate" (90 % ≤ rH ≤ 110 %) and "flooded" (rH > 110 %) is introduced.
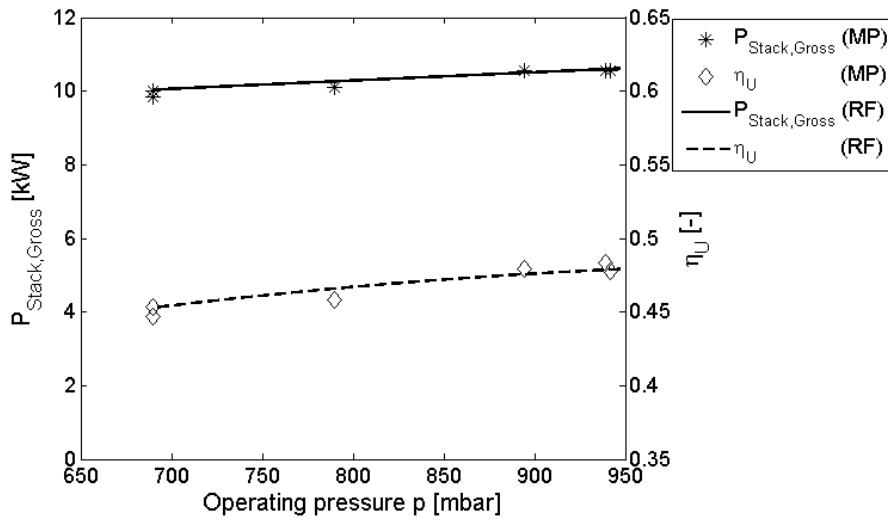
Fig. 6 Gross stack performance and efficiency in PEMFC operation
(reference: t = 45 °C; λ = 2.1; I = 300 A); MP: measuring point; RF: regression function

Tab. 5 Parameters in PEMFC operation (reference: t = 45 °C; λ = 2.1; I = 300 A)

p_cathode_in (measured)	p_cathode_out (measured)	p_w (calculated)	t_cathode_out (measured)	t_dew (calculated)	rH (calculated)	fuel cell humidification
Pa	Pa	Pa	°C	°C	%	-
68971	56600	10882	45.1	47.2	114	flooded
68970	56702	10902	45.1	47.2	114	flooded
78974	67995	13073	45.0	50.9	136	flooded
89423	79308	15248	45.0	54.2	159	flooded
94197	84602	16266	45.0	55.7	170	flooded
93926	84799	16304	45.0	55.7	170	flooded

In addition, the correlation between auxiliary energy demand (BOP: balance of plant) and operating pressure is to be considered [3]. However, Figure 7 proves no significant variation of the auxiliary energy demand for the operating pressure variation at the reference point. The variation of the auxiliary energy demand is 6.1 W for the pressure difference regarded in Figure 7. The standard deviation amounts to 4.34 W (P_{BOP}).
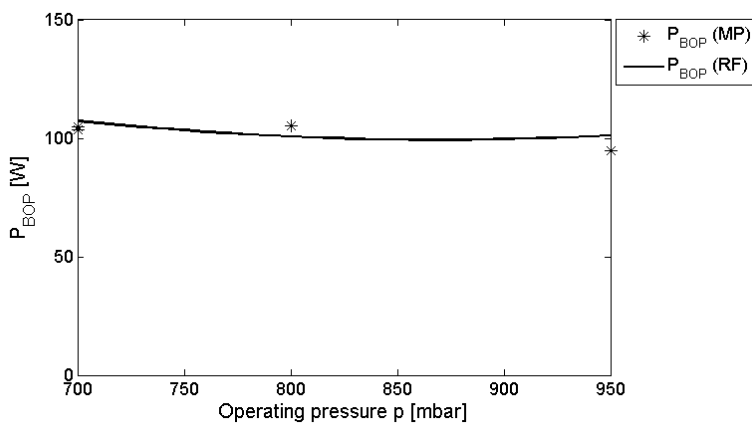

Fig. 7 Auxiliary energy demand in PEMFC operation (reference: t = 45 °C; λ = 2.1; I = 300 A);
MP: measuring point; RF: regression function

3.3. Indexing of operating parameters

Figure 8-10 illustrate the impact of cooling temperature, stoichiometry and load requirement on the gross stack performance and efficiency in fuel cell operation at $p \leq p_{amb.}$.

Figure 8 a-c shows the gross stack performance and efficiency of the fuel cell system at varying operating pressures and fuel cell temperatures. Experimental results as well as corresponding regression functions are included. A variation of the operating pressure from p = 950 mbar to p = 700 mbar results in a decrease in gross stack performance and efficiency of 5.3-16.6 % for cooling temperatures t = 45-55 °C. A decrease of gross stack performance and efficiency of 7.2 % is determinable for a cooling temperature of 65 °C and a reduction of the operating pressure level from p = 950 mbar to p = 900 mbar. A standard deviation of 283.9 W (gross stack performance) and 0.0121 (efficiency) is ascertained. Thus, the specific interest of the cooling temperature to the performance of the fuel cell is confirmed as described in [5, 15, 17-18]. Figure 8 a-b shows increased differential quotients of the regression curve for increasing cooling temperatures at the stack output. The maximal gross stack performance can be achieved by setting the cooling temperature in dependence of the operating pressure. A decrease in operating pressure tends to result in a decreased cooling temperature required to achieve the optimal gross stack performance and efficiency. The optimal cooling temperature (stack output) is t* = 48.4 °C for p = 700 mbar or t* = 52.9 °C for p = 950 mbar according to the mathematical model for evaluation of experiments applied.

The resulting fuel cell humidification at operating parameters defined helps to explain this effect. Table 6 [3)] presents the measured values of pressures p_cathode_in, p_cathode_out and temperature t_cathode_out as well as the corresponding water vapor pressure p_w and the dew point temperature t_dew calculated. Referred to Table 6 all humidification states (dry, adequate, flooded) are represented within steady fuel cell operation. The dew point temperature of the cathode exhaust gas is about 47 °C at 700 mbar. This result accords well with the optimal cooling temperature (stack output) t* = 48.4 °C calculated on the basis of the mathematical model. The dew point temperature of about 56 °C at 950 mbar in Table 6 tends to agree with the respective calculated optimum based on the mathematical model as well.

[3)] Table 6-8 consider measuring points characterized by the operating pressure p_cathode_in ≈ 700 mbar or 950 mbar.
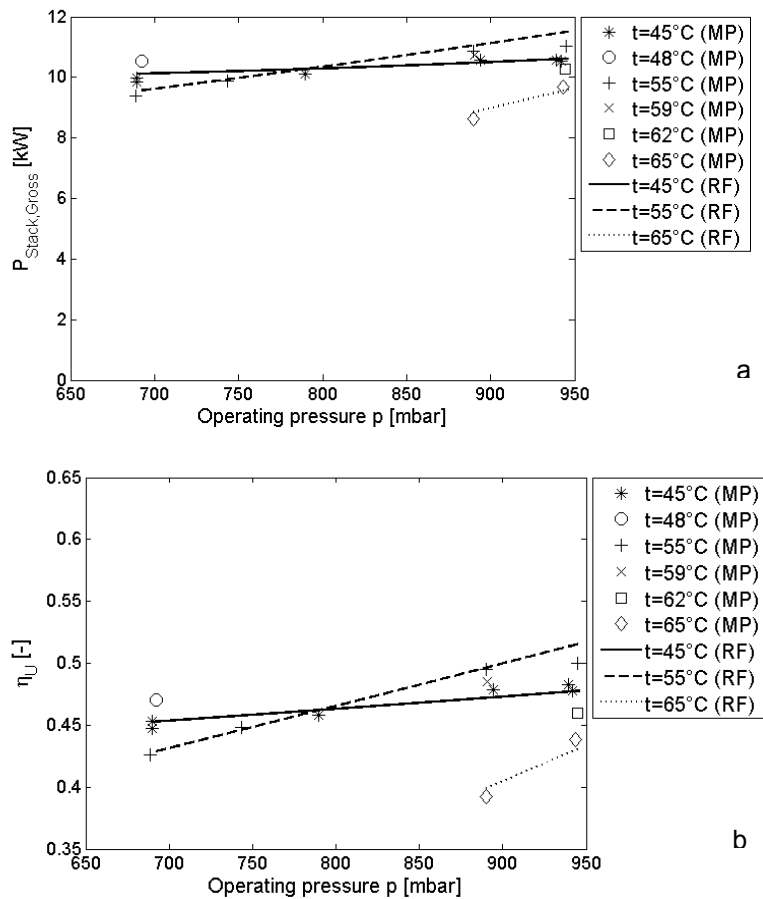
Fig. 8 Gross stack performance (a) and efficiency (b) depending on operating pressure and cooling temperature (reference: λ = 2.1; I = 300 A); MP: measuring point; RF: regression function

Tab. 6 Parameters in PEMFC operation depending on operating pressure and cooling temperature (reference: λ = 2.1; I = 300 A)

p_cathode_in (measured)	p_cathode_out (measured)	p_w (calculated)	t_cathode_out (measured)	t_dew (calculated)	rH (calculated)	fuel cell humidification
Pa	Pa	Pa	°C	°C	%	-
68870	56748	10910	55.0	47.3	69	dry
68970	56702	10902	45.1	47.2	114	flooded
68971	56600	10882	45.1	47.2	114	flooded
69214	57194	10996	48.0	47.4	99	adequate
74339	63234	12157	55.0	49.4	77	dry
93926	84799	16304	45.0	55.7	170	flooded
94197	84602	16266	45.0	55.7	170	flooded
94335	85769	16490	65.0	56.0	66	dry
94460	85995	16533	63.0	56.1	72	dry
94468	85767	16490	55.0	56.0	105	adequate

Figure 9 a-b describes the gross stack performance and efficiency of the fuel cell system depending on the operating pressures and cathode stoichiometric ratios investigated. Experimental results as well as corresponding regression functions are considered. A decrease of 7.2-4.0 % in gross stack performance and efficiency is ascertainable for an operating pressure reduction from p = 950 mbar to p = 700 mbar at cathode

stoichiometric ratios 1.7 ≤ λ ≤ 2.5. The standard deviation accounts for 332.9 W (gross stack performance) and 0.014 (efficiency). However, Figure 9 a-b prove a minor impact of cathode stoichiometric ratios on gross stack performance and efficiency, illustrated by means of the similar differential quotients of the regression functions at reference point defined. Table 7 summarizes cathode stoichiometric ratio, pressures p_cathode_in, p_cathode_out and temperature t_cathode_out, corresponding water vapor pressure p_w and dew point temperature t_dew as well as information related to the fuel cell humidification. With respect to Table 7, all measuring points are characterized by cell flooding. In consequence, there are no significant variations of gross stack performance and efficiency expected due to the water balance of the PEMFC. Thus, the characteristic is to be assigned to the oxygen partial pressure. On this account, the consideration of cell humidification adjusted by the cooling temperature is recommended for further studies on gross stack performance and efficiency at varying operating pressure and/or cathode stoichiometric ratio. According to previous studies [6, 11-12] an increase of gross stack performance and efficiency is predicted in PEMFC operation characterized by increased cathode stoichiometric ratios.
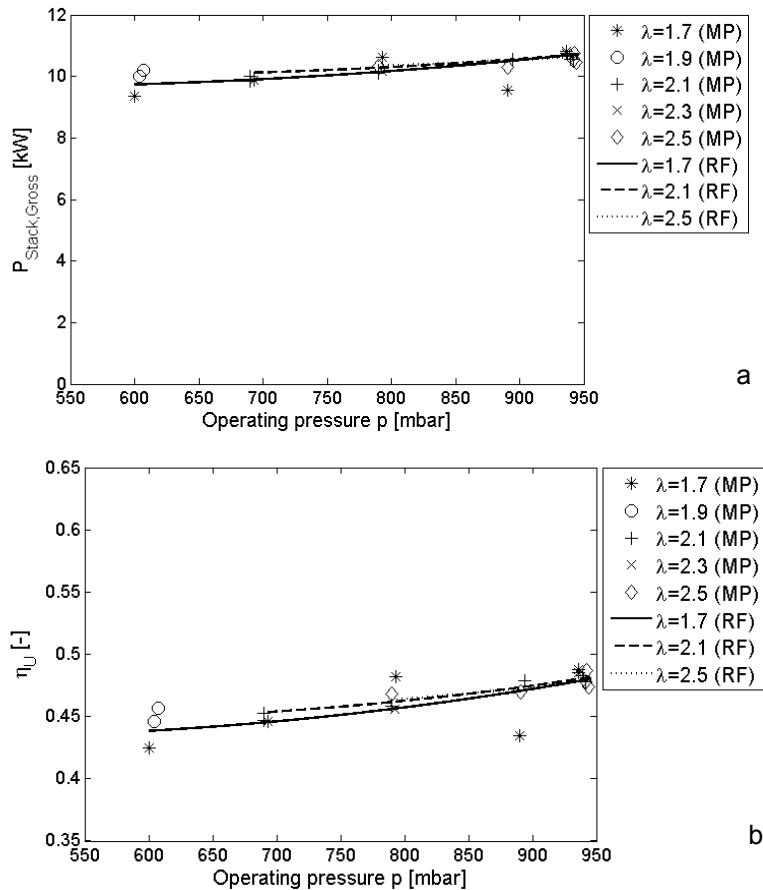

Fig. 9 Gross stack performance (a) and efficiency (b) depending on operating pressure and cathode stoichiometric ratio (reference: t = 45 °C; I = 300 A) ; MP: measuring point; RF: regression function

Tab. 7 Parameters in PEMFC operation depending on operating pressure and cathode stoichiometric ratio
(reference: t = 45 °C; I = 300 A)

cathode stoichiom. ratio	p_cathode _in (measured)	p_cathode _out (measured)	p_w (calculated)	t_cathode _out (measured)	t_dew (calculated)	rH (calculated)	fuel cell humidification
-	Pa	Pa	Pa	°C	°C	%	-
2.1	68970	56702	10902	45.1	47.2	114	flooded
2.1	68971	56600	10882	45.1	47.2	114	flooded
1.7	69333	55967	12836	45.0	50.5	134	flooded
1.7	93613	86523	19870	45.0	60.3	207	flooded
1.7	93624	86485	19861	45.0	60.3	207	flooded
2.1	93926	84799	16304	45.0	55.7	170	flooded
2.5	94169	82539	13695	45.0	51.9	143	flooded
2.1	94197	84602	16266	45.0	55.7	170	flooded
2.5	94271	82599	13705	45.3	51.9	143	flooded
2.5	94418	82610	13707	45.1	51.9	143	flooded

Figure 10 a-b exemplifies gross stack performance and efficiency depending on operating pressure and load requirements of the fuel cell system. Experimental data and corresponding regression function are illustrated. An operating pressure variation 950 mbar ≥ p ≥ 700 mbar at load requirements 300 A ≥ I ≥ 50 A results in a decrease of gross stack performance and efficiency of 1.4 - 5.3 %, according to Figure 10 a-b. The standard deviation is 113.7 W (gross stack performance) and 0.006 (efficiency). Variations of the gross stack performance and efficiency at operating pressures 950 mbar ≥ p ≥ 700 mbar and load requirements 300 A ≥ I ≥ 50 A are rather to be assigned to the impact of oxygen partial pressure, since cell flooding is identified for all measuring points (cp. Table 8). The changes of gross stack performance and efficiency at varying load requirement are characterized by ohmic losses mainly. Significant differences of the resulting differential quotients of the load requirements are not ascertainable.

Further studies to improve load-based fuel cell operation in low pressure environment require an adjustment of cooling temperature and/or cathode stoichiometric ratio to achieve an adequate fuel cell humidification. Detailed investigations on water balance considering the water net drag characteristics in operation of PEMFC will complete the studies.
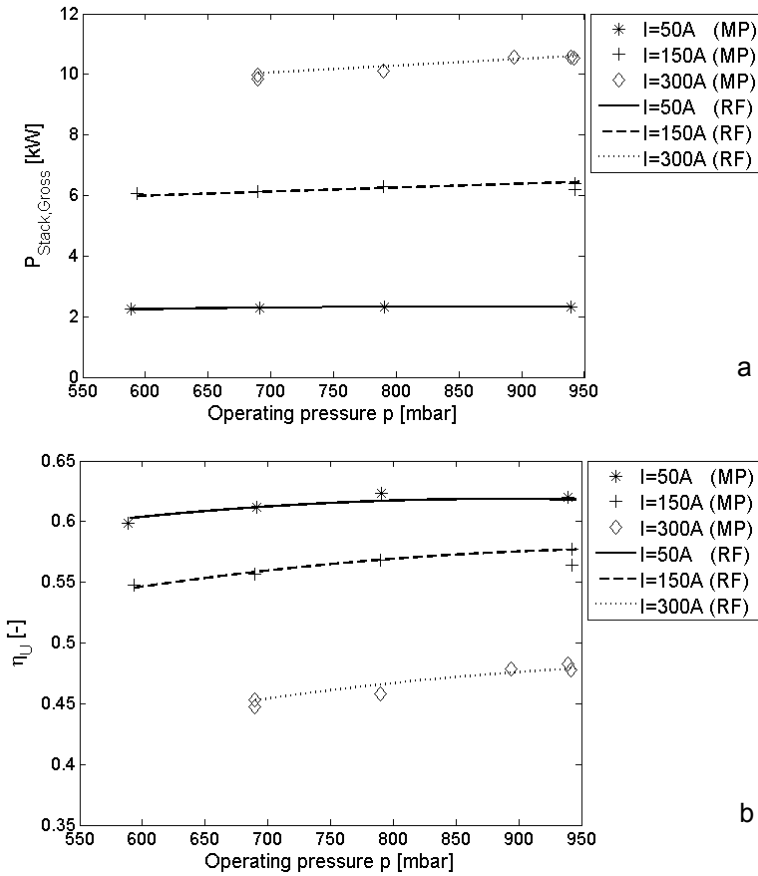
Fig. 10 Gross stack performance (a) and efficiency (b) depending on operating pressure and load requirement (reference: t = 45 °C; λ = 2.1); MP: measuring point; RF: regression function

Tab. 8 Parameters in PEMFC operation depending on operating pressure and load requirement (reference: t = 45 °C; λ = 2.1)

FC current (measured) A	p_cathode _in (measured) Pa	p_cathode _out (measured) Pa	p_w (calculated) Pa	t_cathode_ out (measured) °C	t_dew (calcu-lated) °C	rH (calcu-lated) %	fuel cell humidification -
149	68958	63625	12233	45.0	49.5	128	flooded
299	68970	56702	10902	45.1	47.2	114	flooded
299	68971	56600	10882	45.1	47.2	114	flooded
51	69142	67578	12993	45.1	50.8	136	flooded
51	93900	93073	17894	45.0	57.9	187	flooded
296	93926	84799	16304	45.0	55.7	170	flooded
299	94197	84602	16266	45.0	55.7	170	flooded
150	94206	90152	17333	45.1	57.1	181	flooded
149	94241	90360	17373	45.0	57.2	181	flooded

To sum up, the present experiments confirm the correlation between the operating pressure variation and the fuel cell voltage and consequently the effect on the gross stack performance and efficiency as discussed in [5-6, 8, 15]. The change of the current-voltage characteristic results from the oxygen partial pressure variation and changes of cell humidification depending on the total operating pressure. The cell humidity of the PEMFC is controllable by temperature and/or cathode stoichiometric ratio adjustments in particular [22-23]. Figure 11 a-b compares the effects of the operating parameter increase at p = 700 mbar and p = p_{amb} = 950

mbar. The reference is the cooling temperature at stack output, the cathode stoichiometric ratio and the load requirement defined in section 3.
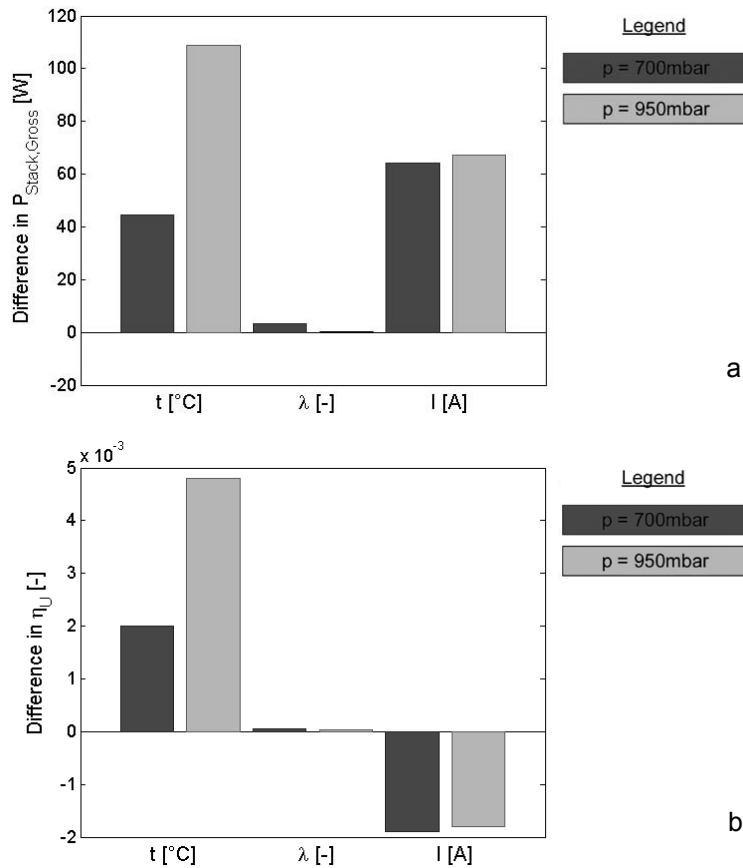

Fig. 11 Effect of a one percent increase per variable each on gross stack performance (a) and efficiency (b) at ambient and low pressure (reference: t = 45 °C; λ = 2.1; I = 300 A)

Figure 11 a-b illustrates minor impact of the cooling temperature on the gross stack performance and efficiency in low pressure operation (p = 700 mbar) compared to ambient pressure operation (p = 950 mbar). Limited gross stack performance and efficiency variations at reference point in low and ambient pressure operation result from modifications of stoichiometry and load requirement.

4. SUMMARY AND OUTLOOK

This paper characterizes ambient pressure operation as well as low pressure operation of a fuel cell system HyPM XR 12 on the basis of experimental analyses. The test procedure and evaluation of the experimental work was realized on the basis of statistical methods. Reference points considering operating pressure, cooling temperature, stoichiometry and load requirement were defined to compare and to rate the experimental results. The following conclusions are to be summarized from the discussion of results:

- There are admissible and non-admissible operating areas in PEMFC operation to be distinguished at ambient and low pressure operation. Especially low operating pressures combined with high cooling temperatures at stack output were not to be realized due to membrane dehumidification. Low operating pressures combined with high stoichiometric ratios or high load requirements were not to be realized at the test facility due to capacity limitations of the vacuum compressor.

- The PEMFC operation at low pressure level (p ≥ 700 mbar) results in a decrease of gross stack performance and efficiency.

- Key factors for gross stack performance and efficiency are oxygen partial pressure and fuel cell humidification, affected by parameters such as cooling temperature, operating pressure and/or cathode stoi-

chiometric ratio. The optimal operating temperature of t*=48.4 °C at p = 700 mbar, λ = 2.1 and t* = 52.9 °C at p = 950 mbar, λ = 2.1 was calculated on the basis of the statistical model introduced for test evaluation.

The German Aerospace Center, Institute of Engineering Thermodynamics will consider the following aspects for further investigations on low pressure operation of PEMFC:

- preparation of a mathematical model to describe the ambient and low pressure operation of PEMFC

- detailed analyses on the effects related to stoichiometry variations at different operating conditions for advanced evaluations of a PEMFC application in aviation. The stoichiometry controls the generation of oxygen depleted air (ODA) to be considered for the multifunctional PEMFC application in aircrafts. Therefore, the variability of ODA generation under specific operating conditions defined at $p \leq p_{amb}$ is to be considered.

- advanced investigations for enhanced load-based fuel cell operation modes in low pressure environment considering operating parameters and water net drag effects for an optimized water management control

Further studies planned on multifunctional fuel cell operation regard the procedural and electric architecture to be expanded and optimized. The integration of a gas drying unit will extent the possibilities for conditioning the oxygen depleted air in fuel cell operation. The advanced design and mode of operation adjusted for multifunctional fuel cell systems will account for an optimal demand oriented PEMFC applications in aviation in medium or long term perspective.

5. ACKNOWLEDGEMENT

REFERENCES

[1] Zeroual, M., et al.: Numerical study of the effect of the inlet pressure and the height of gas channels on the distribution and consumption of reagents in a fuel cell (PEMFC), In: Energy Procedia 18 (2012), pp. 205-214.

[2] Pratt, J. W., et al.: Performance of proton exchange membrane fuel cell at high-altitude conditions, In: Journal of Propulsion and Power, Vol. 23, No. 2, March-April 2007.

[3] Haraldsson, K. et al.: Effects of ambient conditions on fuel cell vehicle performance, In: Journal of Power Sources 145 (2005), pp. 298-306.

[4] Misran, E., et al.: Water transport characteristics of a PEM fuel cell at various operating pressures and temperatures, In: International Journal of Hydrogen Energy (in press).

[5] Santarelli, M. G.: Experimental analysis of the effects of the operating variables on the performance of a single PEMFC, In: Energy Conversion and Management 48 (2007), pp. 40-51.

[6] Horde, T.: PEMFC application for aviation: Experimental and numerical study of sensitivity to altitude, In: International Journal of Hydrogen Energy 37 (2012), pp. 10818-10829.

[7] Murthy, M. et al.: The effect of temperature and pressure on the performance of a PEMFC exposed to transient CO concentrations, In: Journal of the Electrochemical Society, 150 (1) A29-A34 (2003).

[8] Larminie, J., et al.: Fuel Cell Systems Explained, West Sussex: John Wiley & Sons Ltd, 2003.

[9] Rossow, C.-C., Wolf, K., Horst, P.: Handbuch der Luftfahrzeugtechnik, München: Carl Hanser Verlag GmbH & Co. KG, 2013.

[10] Kurzweil, P.: Brennstoffzellentechnik – Grundlagen, Komponenten, Systeme, Anwendungen, Wiesbaden: Friedr. Vieweg & Son Verlag/GWV Fachverlag GmbH, 2003.

[11] Santarelli, M. G., et al.: Experimental analysis of cathode flow stoichiometry on the electrical performance of a PEMFC stack, In: International Journal of Hydrogen Energy 32 (2007) pp. 710-716.

[12] Kim, S. et al.: The effect of stoichiometry on dynamic behavior of a proton exchange membrane fuel cell (PEMFC) during load change, In: Journal of Power Sources 135 (2004), pp. 110-121.

[13] Chu, D. et al.: Performance of polymer electrolyte membrane fuel cell (PEMFC) stacks – Part 1. Evaluation and simulation of an air-breathing PEMFC stack, In: Journal of Power Sources 83 (1999), pp. 128-133.

[14] Jiang, R., et al.: Stack design and performance of polymer electrolyte membrane fuel cells, In: Journal of Power Sources 93 (2001), pp. 25-31.

[15] Amirinejad, M., et al.: Effects of operating parameters on performance of a proton exchange membrane fuel cell, In: Journal of Power Sources 161 (2006), pp. 872-875.

[16] Mallant, R. K. A. M.: PEMFC systems: the need for high temperature polymers as a consequence of PEMFC water and heat management, In: Journal of Power Sources 118 (2003), pp. 424-429.

[17] Hinds, G., et al.: Novel in situ measurements of relative humidity in a polymer electrolyte membrane fuel cell, In: Journal of Power Sources 186 (2009), pp. 52-57.

[18] Zhang, J. et al.: PEM fuel cells operated at 0 % relative humidity in the temperature range of 23-120 °C, In: Electrochimica Acta 52 (2007), pp. 5095-5101.

[19] Ericsson, L., et al.: Design of Experiments: Principles and Applications, Learnways AB, Umea, 2000, pp. 219-220.

[20] Matlab Version 2014 http://www.mathworks.com

[21] Matlab version 2007b, http://www.mathworks.com

[22] Berning, T.: The dew point temperature as a criterion for optimizing the operating conditions of proton exchange membrane fuel cells, In: International Journal of Hydrogen Energy 37 (2012), pp. 10265-10275.

[23] Werner, C., Busemeyer, L., Kallo, J.: The impact of operating parameters and system architecture on the water management of a multifunctional PEMFC system, In: Proceedings of the World Hydrogen Energy Conference 2014.

[24] VDI-Gesellschaft Verfahrenstechnik und Chemieingenieurwesen (Hrsg.): VDI-Wärmeatlas, Berlin, Heidelberg: Springer-Verlag, 2010.

APPENDIX

Main effects and interactions are considered in the design of experiments. Main effects of first (linear), second (quadratic), third (cubic) and fourth (biquadratic) order are those summands that include only one input variable in the first to fourth order. First order interactions include products of two input variables; second order interactions include products of three input variables and so on. Nonlinear effects are those products, which include at least one input variable quadratically. The presented model considers every summand up to the third order as well as biquadratic main effects and third degree interactions. The remaining nonlinear interactions belonging to fourth order are excluded from the model. The quadruplets shown in Table 9 and Table 10 are the exponents of the operating parameters λ, t, p and I in the model function

$$(10) \quad Y = \sum_{j=1}^{n} \beta_j \cdot \lambda^{j1} \cdot t^{j2} \cdot p^{j3} \cdot I^{j4}$$

Y represents the target variable, β_j the model coefficients and $j_1 - j_4$ the exponents shown in Table 9 and Table 10.

Example: The effect 1200 (cp. Table 10, 1st line, 4th column) is written in the model function as

$$(11) \quad Y = \beta_j \cdot \lambda^1 \cdot t^2 \cdot p^0 \cdot I^0 = \beta_j \cdot \lambda^1 \cdot t^2$$

Tab. 9 Definition of the main effects and constants

constant	linear	quadratic	cubic	biquadratic
$j_1\ j_2\ j_3\ j_4$	$j_1\ j_2\ j_3\ j_4$	$j_1\ j_2\ j_3\ j_4$	$j_1\ j_2\ j_3\ j_4$	$j_1\ j_2\ j_3\ j_4$
0000	1000	2000	3000	4000
	0100	0200	0300	0400
	0010	0020	0030	0040
	0001	0002	0003	0004

Tab. 10 Definition of the interactions (IA)

interaction 1st order	interaction 2nd order	interaction 3th order	non-linear interaction
$j_1\,j_2\,j_3\,j_4$	$j_1\,j_2\,j_3\,j_4$	$j_1\,j_2\,j_3\,j_4$	$j_1\,j_2\,j_3\,j_4$
1100	1110	1111	1200
1010	1101		1020
1001	1011		1002
0110	0111		0120
0101			0102
0011			0012
			2001
			2010
			2100
			0210
			0201

All areas depicted row wise in Table 11 are excluded from the experimental design as non-admissible operating fields, since a steady operation at the low pressure fuel cell test facility was not to be realized.

Tab. 11 Overview of the non-admissible areas

λ [-]	t [°C]	p [mbar]	I [A]
	≤ 50		≥350
	≥65	≤800	
	≥65		≤150
≤1.7			≤50/≥350
≤1.7	≥55	≤600	≥250
≤1.7	≥60	≤700	≥150
≤1.9		≤600	≥350
≤1.9	≥60	≤700	≥350
≤1.9	≥60	≤600	
≥2.1	≥60	≤700	
≥2.1		≤600	≥300
≥2.1		≤700	≥350
≥2.3	≥65	≤900	
≥2.3	≥50	≤600	≥250
≥2.5		≤600	≥250
≥2.5		≤800	≥350
≥2.5		≤700	≥300